Particle Accelerators, 1990, Vol. 34, pp. 131–154
Reprints available directly from the publisher
Photocopying permitted by license only

Printed in the United States of America

QUASI-WAKE FUNCTION FOR ANALYSIS OF INTERACTIONS BETWEEN CHARGED PARTICLES AND WAKE FIELDS

KENJI MIYATA and MASATSUGU NISHI

Energy Research Laboratory, Hitachi, Ltd. 1168 Moriyama-cho, Hitachi-shi, Ibaraki-ken, 316 Japan

(Received April 3, 1989)

In order to reduce the computing time required for obtaining the wake function (Green's function), an approximate wake function, designated a *quasi-wake function,* is presented, which accurately generates the wake potential for a finite particle distribution. Below a critical frequency, the quasi-wake function has a Fourier component in agreement with that of the exact wake function within a computational error of 0.1%. The computing time required for obtaining the quasi-wake function can be reduced by a factor of about 600 in a two-dimensional wake field analysis, and about 5600 in a three-dimensional wake field analysis, compared with a conventional short-bunch method. The quasi-wake function is also applicable to calculation of coupling impedances of rf cavities.

1. INTRODUCTION

Performance of high-current electron accelerators depends on the single-bunch instabilities that result from interactions between charged particles and self-induced wake fields. Stability analysis requires a wake function to provide information on short-range wake fields—that is, the transient electromagnetic fields that occur inside the electron bunch due to the interaction between the bunch itself and the surroundings. The wake function has longitudinal and transverse components. The two components have singularities[1] peculiar to the Green's function at the origin, where the first-order differential coefficient of the longitudinal wake function and the second-order differential coefficient of the transverse one have infinite values. Therefore, the wake functions have a great many high-frequency components. Obtaining a more accurate wake function requires more of the high frequency components, i.e., a smaller mesh size in the finite mesh code for computing wake fields or rf electromagnetic fields. Consequently, the computations are time-consuming and require enormous amounts of memory.

From the viewpoint of a theoretical or a particle-tracking analysis of beam instabilities, the final target of wake field analysis is not the accurate wake function, but rather the accurate wake *potential* inside the finite bunch. Since no finite-mesh code can calculate the exact wake function due to the singularity at the origin, it is better to use an approximate kernel function of the convolution integral equation as the wake function, which gives the wake potential inside the

finite bunch with less computational error. In this paper, the kernel function is designated a *quasi-wake function,* which is obtained by eliminating the high-frequency components, which have little effect on the wake potential.

In Section 2, conventional methods are reviewed; this motivated the development of the quasi-wake function. In Section 3, the quasi-wake function is derived, and its applicability and effectiveness are shown from the viewpoints of bunch length and computing time. Next, Section 4 applies the method of the quasi-wake function to a reentrant rf cavity. In Section 5, the analysis method of coupling impedances is illustrated by making use of the Fourier transform of the quasi-wake function, and it is applied to the reentrant cavity. The results are compared with those obtained from the well-known electromagnetic field analysis code SUPERFISH.[2]

2. CONVENTIONAL METHODS

Before reviewing the conventional methods, the wake potential is described briefly. The wake potential $\mathbf{W}(T)$ is defined in the following vector form:[3]

$$\mathbf{W}(T) = \int_L [\mathbf{E}(z, T') + \mathbf{v}(z, T') \times \mathbf{B}(z, T')]\, dz, \tag{1}$$

with

$$T = ct; \tag{2}$$

$$T' = \frac{T + z}{\beta}; \tag{3}$$

and

$$\beta = \frac{|\mathbf{v}|}{c} \tag{4}$$

Here $\mathbf{E}$ and $\mathbf{B}$ are the electric and magnetic components of the wake field, $\mathbf{v}$ is the particle velocity; L, the effective domain of the wake field; c, the light velocity; t, the time; and z, the longitudinal coordinate along the particle trajectory. When the velocity $\mathbf{v}$ is nearly constant, the wake potential is nearly proportional to the change of the particle's momentum due to the electromagnetic forces of the wake fields. Under the linearity of the wake field, each component of the wake (vector) potential is expressed as the following convolution-integral form of the current distribution $I(T)$ of the electron bunch and the wake function $W_\delta(T)$, which is often referred to as a delta-function wake potential;

$$W(T) = \frac{1}{c} \int_{-\infty}^{\infty} I(T') W_\delta(T - T')\, dT'. \tag{5}$$

The wake function enables calculation of the wake potentials for an arbitrary current distribution.

The wake function can be approximately given by the short-bunch method[4] or the mode summation method[5] using the optical resonator model.[5,6] In the former

method, the wake function is approximated as the wake potential by the short bunch with a Gaussian current distribution, which is designated here as a reference Gaussian bunch. In the latter method, the wake function is composed of a great many resonant modes over a wide frequency range. The validity of this method was first pointed out by Bane.[7]

2.1. *Short-Bunch Method*

A Gaussian bunch longer than the reference Gaussian bunch induces a wake potential $W_g(T)$ expressed exactly as [8]

$$W_g(T) = \frac{1}{(2\pi)^{1/2}\sigma_0} \int_{-\infty}^{\infty} \exp\left(-\frac{T'^2}{2\sigma_0^2}\right) W_r(T - T')\, dT'. \tag{6}$$

with

$$\sigma_0 = (\sigma_g^2 - \sigma_r^2)^{1/2}; \tag{7}$$

where σ_g and σ_r are the rms lengths of the Gaussian bunch and the reference Gaussian bunch, respectively, and $W_r(T)$ is the wake potential of the reference Gaussian bunch (reference wake potential). In the short-bunch method, the reference wake potential $W_r(T)$ is substituted for the wake function $W_\delta(T)$, and therefore the wake potential $W_g(T)$ is approximately expressed as

$$W_g(T) = \frac{1}{(2\pi)^{1/2}\sigma_g} \int_{-\infty}^{\infty} \exp\left(-\frac{T'^2}{2\sigma_g^2}\right) W_r(T - T')\, dT'. \tag{8}$$

Eqs. (6) and (8) differ in the terms σ_0 and σ_g, which gives rise to a significant error in the case of $\sigma_g \fallingdotseq \sigma_r$. No problem is caused by using Eq. (6) in the case of the Gaussian bunch. In the case of the general particle distribution in the bunch with the rms bunch length σ, however, the application of the short-bunch method is limited to long bunches with $\sigma^2 \gg \sigma_r^2$ ($\sigma \gtrsim 5\sigma_r$).

2.2. *Mode Summation Method*

The mode summation method is based on another expression[6] of the wake function, written as follows:[9]

$$W(T) = -2U(T) \sum_{n=1}^{\infty} \kappa_n \exp(-\alpha_n K_n T)[\cos(K_n T) - \alpha_n \sin(K_n T)], \tag{9}$$

with

$$\alpha_n = \frac{1}{2S_n Q_n}; \tag{10}$$

$$\kappa_n = \frac{\omega_n}{2}\left(\frac{R_n}{Q_n}\right) \quad \text{(loss parameter)}; \tag{11}$$

$$\omega_n = k_n c; \tag{12}$$

$$K_n = S_n k_n; \tag{13}$$

$$S_n = \left(1 - \frac{1}{4Q_n^2}\right)^{1/2}; \tag{14}$$

$U(T)$: Heaviside step function;

k_n: wave number of resonant mode n;

R_n: coupling impedance of resonant mode n;

and

Q_n: quality factor of resonant mode n.

Eq. (9) is given by the inverse Fourier transform of the following coupling impedance $Z(k)$:

$$Z(k) = \sum_{n=1}^{\infty} \frac{R_n}{1 + jQ_n\left(\frac{k}{k_n} - \frac{k_n}{k}\right)}. \tag{15}$$

It is impractical to calculate Eq. (9) since the density of the modes increases in proportion to frequency.[10] In order to put the mode summation method to practical use, the optical resonator model[5,6] is applied to disk-loaded cavities as an analytical extension in the following form:

$$W(T) = -2U(T)\left[\sum_{n=1}^{N} \kappa_n \cos(k_n T) + \int_{k_{N+1}}^{\infty} \kappa \frac{dn}{dk} \cos(kT)\, dk\right], \tag{16}$$

with

$$\kappa \frac{dn}{dk} = \frac{c}{2} C_{sv} F_a(k/k_a) F_b(k/k_b); \tag{17}$$

$$F_a(x) = \frac{x^{1/2} + 1}{[(x^{1/2} + 1)^2 + 1]^2}; \tag{18}$$

$$F_b(x) = x^2 K_1^2(x); \tag{19}$$

$$k_a = 0.170 \frac{d}{a^2}; \tag{20}$$

$$k_b = \frac{\beta}{a(1 - \beta^2)^{1/2}}; \tag{21}$$

$$C_{sv} = \frac{650}{\beta}(\Omega) \quad \text{(Sessler-Vainshtein constant)}; \tag{22}$$

and where a is the beam tube radius; d, the gap length; k_{N+1}, the wave number of the resonant mode $N + 1$; and $K_1(x)$, the first-order modified Bessel function of the first kind. However, the analytical extension assumes that the cavities under consideration are in an infinite periodic structure, and that every mode has an infinite quality factor. The analytical extension is not applicable to a finite number of cavities connected to beam tubes on both sides, the quality factor of which is on the order of unity above the cutoff frequency determined by the beam tube radius because of high-frequency field dissipation to the beam tubes.

3. QUASI-WAKE FUNCTION

3.1. Derivation

The symbols used here are summarized in Table 1. When the current distribution $I(T)$ equals the current distribution $I_r(T)$ of the reference Gaussian bunch, Eq. (5) leads to the following expression in the frequency domain:

$$Z_r(k) = \tilde{I}_r(k)Z(k), \tag{23}$$

where

$$Z_r(k) = -\frac{1}{c}\int_{-\infty}^{\infty} W_r(T)e^{-jkT}\,dT; \tag{24}$$

TABLE I

Symbols and Their Definitions

Symbol	Definition
$W_\delta(T)$	Wake function
$\hat{W}_\delta(T)$	Quasi-wake function
$W_r(T)$	Reference wake potential
$Z(k)$	Coupling impedance
$\tilde{Z}(k, k_c)$	Quasi-coupling impedance without window
$\hat{Z}(k, k_c; k_I, k_G)$	Quasi-coupling impedance where the function $G(T, k_c)$ is multiplied by a Hanning-type window and the reference current distribution $I_r(T)$ is multiplied by a box-type window
$Z_c(k)$	Coupling impedance obtained by finite Fourier transform of wake function in Eq. (70a)
$\hat{Z}_c(k)$	Coupling impedance obtained by finite Fourier transform of the wake function multiplied by the Hanning-type window in Eq. (76a)
k_c	Critical wave number
f_c	Critical frequency
σ_r	RMS bunch length of reference Gaussian bunch
q	Total charge of reference Gaussian bunch
$G(T, k_c)$	Kernel function for generating quasi-wake function
$G_b(T, k_c; T_G)$	$G(T, k_c)$ multiplied by a box-type window
$G_h(T, k_c; T_G)$	$G(T, k_c)$ multiplied by a Hanning-type window
$\tilde{G}(k, k_c)$	Fourier transform of $G(T, k_c)$
$\tilde{G}_b(k, k_c; k_G)$	Fourier transform of $G_b(T, k_c; T_G)$
$\tilde{G}_h(k, k_c; k_G)$	Fourier transform of $G_h(T, k_c; T_G)$
$H_b(T, T_G)$	Box-type window
$H_h(T, T_G)$	Hanning-type window
$\tilde{H}_b(k, k_G)$	Fourier transform of $H_b(T, T_G)$
$\tilde{H}_h(k, k_G)$	Fourier transform of $H_h(T, T_G)$
$I_r(T)$	Reference current distribution
$\tilde{I}_r(k)$	Fourier transform of $I_r(T)$
$\hat{I}_r(k)$	Fourier transform of $I_r(T)$ multiplied by a box-type window
T_G	Maximum value of truncated domain of integration in Eq. (31a)
ξ_G	Maximum value of truncated domain of integration in Eq. (31b)

$$\tilde{I}_r(k) = \frac{1}{c}\int_{-\infty}^{\infty} I_r(T)e^{-jkT}\,dT; \tag{25}$$

$$Z(k) = -\frac{1}{c}\int_{-\infty}^{\infty} W_\delta(T)e^{-jkT}\,dT; \tag{26}$$

and $W_r(T)$ is the wake potential induced by the reference Gaussian bunch with the current distribution $I_r(T)$.

Next, the shapes of the functions $\tilde{I}_r(k)$ and $Z(k)$ should be noted. The current distribution $I_r(T)$ is written as:

$$I_r(T) = \frac{qc}{(2\pi)^{1/2}\sigma_r}\exp\left(-\frac{T^2}{2\sigma_r^2}\right), \tag{27}$$

where q is the total charge in the bunch. Through a Fourier transform the current distribution $I_r(T)$ of the reference Gaussian bunch becomes:

$$\tilde{I}_r(k) = q\exp(-\sigma_r^2 k^2/2). \tag{28}$$

Typical shapes of the functions $Z(k)$, $\tilde{I}_r(k)$ and $Z_r(k)$ are shown in Fig. 1, which

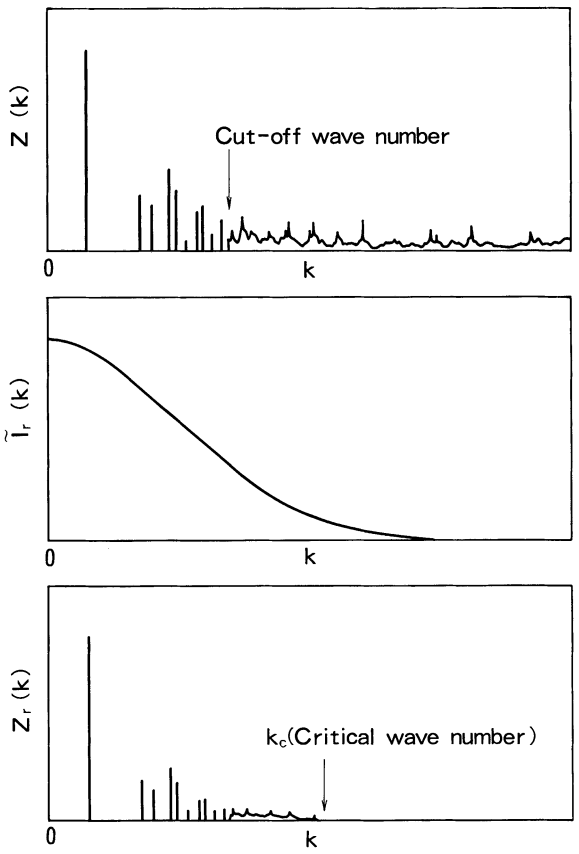

FIGURE 1 Typical shapes of the functions $Z(k)$, $\tilde{I}_r(k)$ and $Z_r(k)$

indicates that $Z_r(k)$ is not affected by the high frequency components of $Z(k)$ above a certain wave number k_c (critical wave number). This means that $Z_r(k)$ is expressed satisfactorily even by the quasi-coupling impedance $\bar{Z}(k, k_c)$ which cuts off all high-frequency components above k_c from the exact coupling impedance $Z(k)$. The quasi-coupling impedance $\bar{Z}(k, k_c)$ is written in the following form:

$$\bar{Z}(k, k_c) = U_f(k, k_c)Z(k), \tag{29}$$

where

$$U_f(k, k_c) = \begin{cases} 1 & (\text{for } |k| \leqq k_c) \\ 0 & (\text{for } |k| > k_c). \end{cases} \tag{30}$$

Here the critical wave number k_c should be selected as a high value so as to provide actual Fourier components of the particle bunch to be analyzed. The quasi-wake function $\hat{W}_\delta(T)$ is defined as the inverse Fourier transform of the quasi-coupling impedance $\bar{Z}(k, k_c)$ in the following form:

$$\hat{W}_\delta(T) = \frac{1}{qc}\int_{-\infty}^{\infty} G(T', k_c)W_r(T - T')\,dT' \tag{31a}$$

$$= \frac{1}{\pi q}\int_{-\infty}^{\infty} g(\xi', u_c)W_r[\xi - \xi']\,d\xi', \tag{31b}$$

where

$$T = \frac{\sigma_r}{2^{1/2}}\xi; \tag{32}$$

$$G(T, k_c) = \frac{2^{1/2}c}{\pi\sigma_r}g(\xi, u_c); \tag{33}$$

$$g(\xi, u_c) = \int_0^{u_c} \exp(u^2)\cos(\xi u)\,du; \tag{34}$$

$$u_c = \frac{\sigma_r k_c}{2^{1/2}}; \tag{35}$$

$$W_r[\xi] = W_r(T). \tag{36}$$

The above derivation indicates that the quasi-wake function $\hat{W}_\delta(T)$ is equivalent to the function derived from the exact wake function $W_\delta(T)$ passed through the low-pass filter with the minimum filtering wave number k_c. The filtering eliminates the singularity peculiar to Green's function at the origin, and the quasi-wake function is not satisfied with the causality condition of having a zero value all over the negative time domain. If the high frequency components of the current distribution are negligible above the critical frequency f_c $(=ck_c/2\pi)$, the dissatisfaction with the causality condition gives a negligible effect on the wake potential obtained from the quasi-wake function.

When analyzing coherent phenomena of particles through the particle tracking analysis by using the wake function, numerical fluctuations[11] appear in the calculated results since the number of super-particles is limited to a value less than the actual number of particles by a factor of $10^6 - 10^{12}$. While the exact wake

function enhances the numerical fluctuations due to the singularity and requires more super-particles and a more time-consuming computation, the quasi-wake function does not enhance the numerical fluctuations because it has no singularity.

3.2. *Method for High-Accuracy Computation*

The computational accuracy of the quasi-wake function depends on T_G or ξ_G, the maximum truncated value of $|T'|$ or $|\xi'|$ in the integral calculation of Eq. (31). Since $G(T, k_c)$ or $g(\xi, u_c)$ is a slowly damping oscillation function, high accuracy in calculation requires a very large domain of integration. Two examples of the function $g(\xi, u_c)$ are shown in Fig. 2 with $u_c = 1.5$ and 2.0, which correspond to $f_c = 2.0$ GHz and 2.7 GHz in the case of $\sigma = 5$ cm. A large value of u_c moderates the damping per oscillation and requires a larger domain of integration. When the

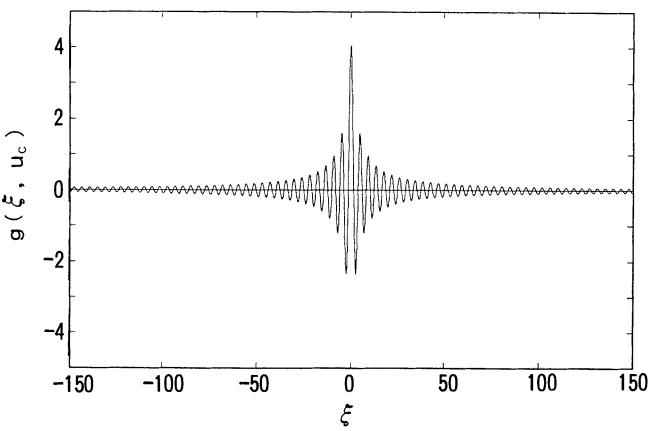

(a) $u_c = 1.5$

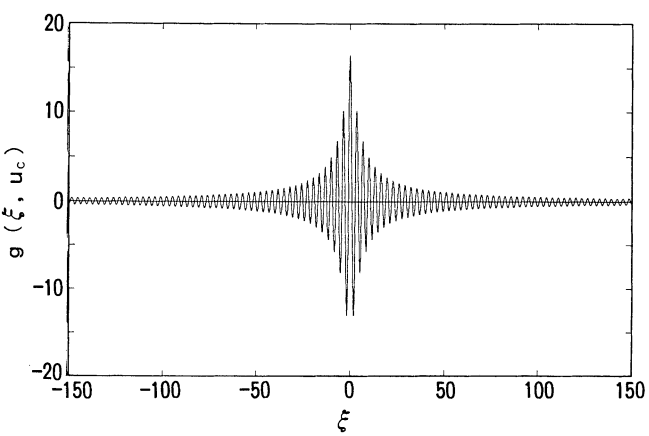

(b) $u_c = 2.0$

FIGURE 2 Function $g(\xi, u_c)$

domain $\{\xi \mid -\infty \leqq \xi \leqq \infty\}$ is limited to $\{\xi \mid -100 \leqq \xi \leqq 100\}$, a computational accuracy of several percent is obtained with $u_c \lesssim 1.5$, but the computational error becomes larger over 20–30% with $u_c \gtrsim 2.0$. The large domain requires a very time-consuming computation of the reference wake potential over a long time range.

The truncated domain $\{T \mid -T_G \leqq T \leqq T_G\}$ is equivalent to multiplying $G(T, k_c)$ by the box-type window $H_b(T, T_G)$ as follows:

$$G_b(T, k_c; T_G) = G(T, k_c) H_b(T, T_G), \tag{37}$$

with

$$H_b(T, T_G) = \begin{cases} 1 & (\text{for } |T| \leqq T_G) \\ 0 & (\text{for } |T| > T_G). \end{cases} \tag{38}$$

In order to reduce the computing time, the following Hanning-type window[12] $H_h(T, T_G)$ is used instead of the box-type window $H_b(T, T_G)$:

$$G_h(T, k_c; T_G) = G(T, k_c) H_h(T, T_G), \tag{39}$$

with

$$H_h(T, T_G) = \begin{cases} F(T/T_G) & (\text{for } |T| \leqq T_G) \\ 0 & (\text{for } |T| > T_G), \end{cases} \tag{40}$$

$$F(x) = \tfrac{1}{2}(1 + \cos(\pi x)). \tag{41}$$

The Fourier components of $G(T, k_c)$, $G_b(T, k_c; T_G)$, $G_h(T, k_c; T_G)$, $H_b(T, T_G)$ and $H_h(T, T_G)$ are defined as $\tilde{G}(k, k_c)$, $\tilde{G}_b(k, k_c; k_G)$, $\tilde{G}_h(k, k_c; k_G)$, $\tilde{H}_b(k, k_G)$ and $\tilde{H}_h(k, k_G)$, respectively, where k_G is defined as

$$k_G = \frac{2\pi}{T_G}. \tag{42}$$

The Fourier transform of Eqs. (37) and (39) takes the following forms:

$$\tilde{G}_b(k, k_c; k_G) = \tilde{G}(k, k_c) * \tilde{H}_b(k, k_G), \tag{43}$$

$$\tilde{G}_h(k, k_c; k_G) = \tilde{G}(k, k_c) * \tilde{H}_h(k, k_G), \tag{44}$$

where $*$ indicates the convolution multiplied by $1/2\pi$.

The two windows $H_b(T, T_G)$, $H_h(T, T_G)$ and their Fourier components $\tilde{H}_b(k, k_G)$ and $\tilde{H}_h(k, k_G)$ are shown in Fig. 3. In the box-type window case, the damping of the spectral oscillation is more moderate with $|k| > k_G$, and $\tilde{G}_b(k, k_c; k_G)$ is affected by the wide range components of $\tilde{G}(k, k_c)$. On the other hand, the spectral oscillation of the Hanning-type window damps rapidly; therefore the Hanning-type window does not distort the spectrum $\tilde{G}(k, k_c)$ as strongly as the box-type window. The superiority of the Hanning-type window is evident in Fig. 4, which shows the frequency dependence of the ratios γ_b and γ_h. They are given by:

$$\gamma_b = \frac{\tilde{G}_b(k, k_c; k_G)}{\tilde{G}(k, k_c)}, \tag{45}$$

$$\gamma_h = \frac{\tilde{G}_h(k, k_c; k_G)}{\tilde{G}(k, k_c)}, \tag{46}$$

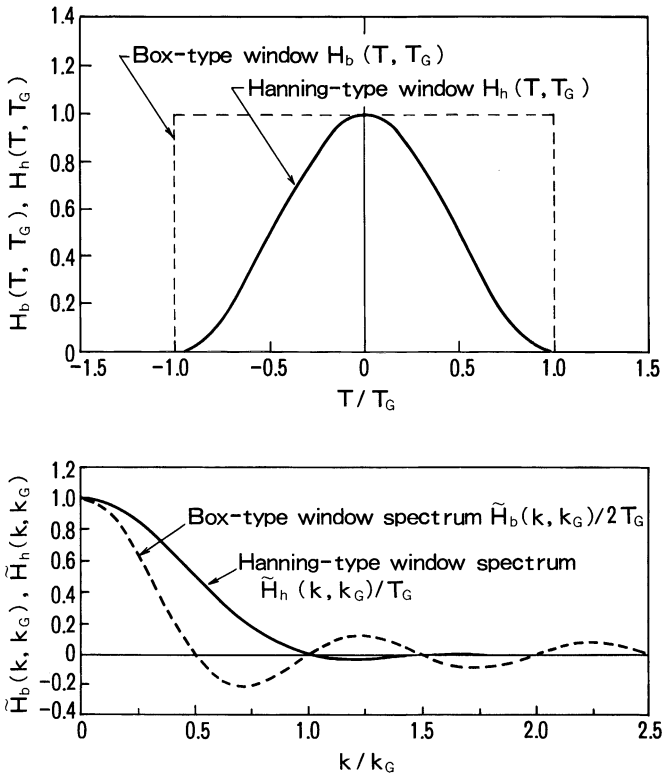

FIGURE 3 Box-type window $H_b(T, T_G)$, Hanning-type window $H_h(T, T_G)$ and their Fourier components $\tilde{H}_b(k, k_G)$ and $\tilde{H}_h(k, k_G)$.

with $\sigma_r = 5$ cm and $f_c = 3$ GHz. The deviation of the ratio from 1.0 is less than 1% in the case of the Hanning-type window, while the maximum deviation is 30% in the case of the box-type window. As shown in this example, the Hanning-type window does not distort the spectrum $\tilde{G}(k, k_c)$ at wave numbers below the vicinity of the critical wave number k_c. It should be noted that the typical width Δk of the window spectrum $\tilde{H}_h(k, k_G)$ and the typical width Δk_0 of spectrum $\tilde{G}(k, k_c)$ satisfy the following relation:

$$\Delta k/\Delta k_0 \ll 1. \tag{47}$$

Here, Δk_0 and Δk are expressed as:

$$\Delta k_0 = \frac{2^{1/2}}{\sigma_r}[u_c - (u_c^2 - \ln 2)^{1/2}], \tag{48}$$

$$\Delta k = \frac{k_G}{2} = \frac{\pi}{T_G} = \frac{\pi 2^{1/2}}{\sigma_r \xi_G}, \tag{49}$$

where Δk_0 is defined as the full width at the half maximum of $\tilde{G}(k, k_c)$. Then Eq.

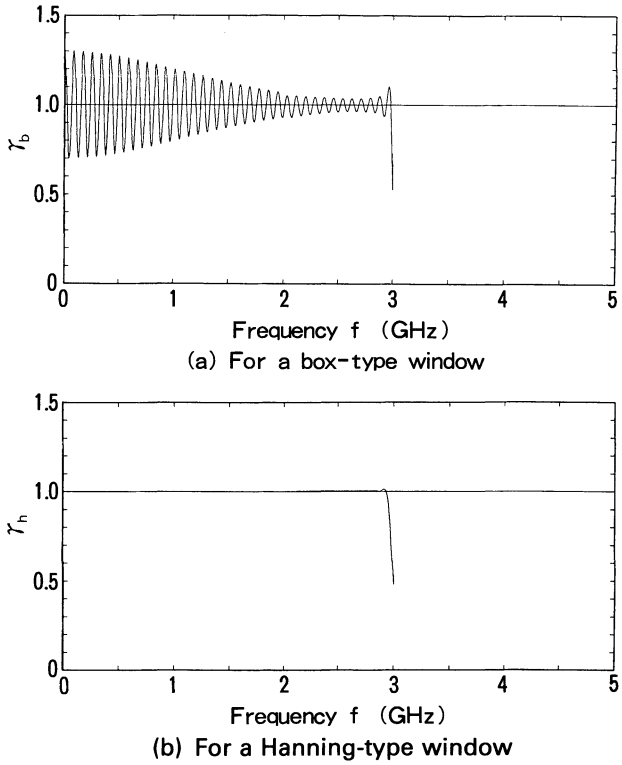

FIGURE 4 Frequency dependence of ratios γ_b and γ_h with $\sigma_r = 5\,\text{cm}$ and critical frequency $f_c = 3\,\text{GHz}$.

(47) is transformed as follows:

$$\xi_g \gg \frac{\pi}{u_c - (u_c^2 - \ln 2)^{1/2}}. \tag{50}$$

Equation (50) indicates that $\xi_0 \gg 19.4$ with $u_c = 2.22$, while $\xi_G = 100$ with the same u_c in Fig. 4.

While the function $G(T, k_c)$ is multiplied by the Hanning-type window $H_h(T, T_G)$ as described above, the reference current distribution function $I_r(T)$ is multiplied by the box-type window $H_b(T, T_I)$. It cannot be multiplied by the same Hanning-type window $H_h(T, T_I)$ as the function $G(T, k_c)$. The reason is that the Hanning-type window remarkably distorts the Fourier component of the current distribution due to the absence of a long oscillating tail as in the function $G(T, k_c)$. This explanation is reasonable considering the residual Fourier component: $\tilde{G}(k, k_c) * (1 - \tilde{H}_h(k, k_G))$.

The quasi-coupling impedance $\hat{Z}(k, k_c; k_I, k_G)$ deduced from the Fourier transform of the quasi-wake function is written in the following form:

$$\hat{Z}(k, k_c; k_I, k_G) = Z(k)(\tilde{I}_r(k) * \tilde{H}_b(k, k_I))(\tilde{G}(k, k_c; k_G) * \tilde{H}_h(k, k_G)), \tag{51}$$

with

$$k_I = \frac{2\pi}{T_I}, \tag{52}$$

where $Z(k)$ is the exact coupling impedance and $\tilde{I}_r(k)$ is the Fourier transform of current distribution function $I_r(T)$. The Fourier component $\hat{I}_r(k)$ of the current distribution function multiplied by the window $H_b(T, T_I)$ is

$$\hat{I}_r(k) = \tilde{I}_r(k) * \tilde{H}_b(k, k_I) \tag{53a}$$

$$= q \exp(-\sigma_r^2 k^2/2) \operatorname{Re}(\Phi(x_2) - \Phi(x_1)), \tag{53b}$$

where $\Phi(x)$ is the complex error function defined as follows:

$$\Phi(x) = \frac{2}{\pi^{1/2}} \int_0^x \exp(-t^2)\, dt, \tag{54}$$

and

$$\operatorname{Re}(x): \text{ real part of complex } x; \tag{55}$$

$$x_1 = j\frac{\sigma_r k}{2^{1/2}}; \tag{56}$$

$$x_2 = \frac{1}{2^{1/2}}(N_\sigma + j\sigma_r k); \tag{57}$$

$$N_\sigma = \frac{T_I}{\sigma_r}. \tag{58}$$

The exact Fourier component $\tilde{I}_r(k)$ of the Gaussian bunch current is:

$$\tilde{I}_r(k) = q \exp(-\sigma_r^2 k^2/2). \tag{59}$$

Therefore, γ_I, the ratio of $\hat{I}_r(k)$ to $\hat{I}_r(k)$, is

$$\gamma_I = \operatorname{Re}(\Phi(x_2) - \Phi(x_1)). \tag{60}$$

The $\sigma_r k$-dependence of γ_I is shown in Fig. 5 with the free parameter N_σ. This

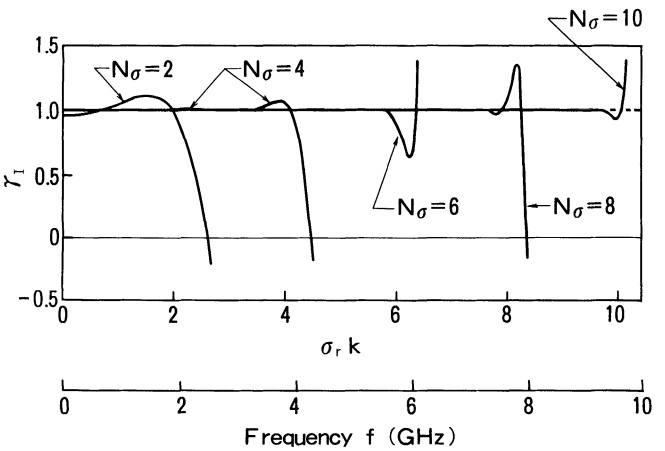

FIGURE 5 $\sigma_r k$-dependence of γ_1 (frequency dependence with $\sigma_r = 5$ cm).

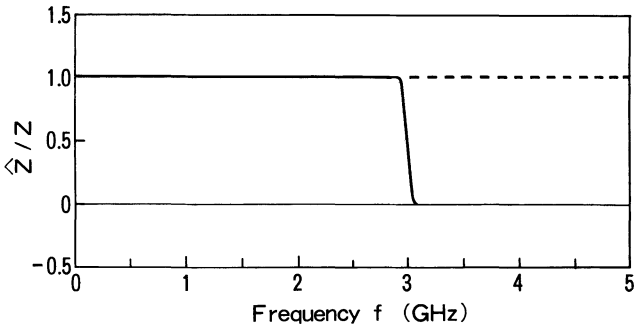

FIGURE 6 Frequency dependence of the ratios of the quasi-coupling impedance $\hat{Z}$ to the exact Z with $\sigma_r = 5$ cm, $f_c = 3$ GHz, and $N_\sigma = 4$.

figure also depicts the equivalent frequency values with $\sigma_r = 5$ cm. This figure indicates that γ_I nearly equals unity with $\sigma_r k \lesssim N_\sigma - 0.5$ when $N_\sigma \gtrsim 4$; that is, the current distribution multiplied by the box-type window can be used without spectrum distortion under this condition. In the case of $\sigma_r = 5$ cm, for example, γ_I nearly equals unity below 3 GHz when $N_\sigma = 4$ or below 5 GHz when $N_\sigma = 6$.

Consequently, the quasi-wake funtion is satisfactorily obtained in the following condition:

$$N_\sigma \gtrsim \max(4, \sqrt{2}\, u_c + 0.5). \tag{61}$$

For example, the frequency dependence of the ratio of the quasi-coupling impedance (Fourier component of quasi-wake function) to the exact one is shown in Fig. 6 with $\sigma_r = 5$ cm, $f_c = 3$ GHz, and $N_\sigma = 4$. This figure explicitly indicates that the quasi-coupling impedance agrees quite well with the exact one below the vicinity of the critical frequency of 3 GHz.

3.3. Applicable Bunch Length and Computing Time

It is important to estimate the relation between the length of the reference Gaussian bunch and that of the particle bunch to which the quasi-wake function is applicable as the approximate kernel function in Eq. (5). Here, the bunch shape is assumed to be a Gaussian distribution. If the wake potential is computed to three significant figures, the applicable rms bunch length σ is

$$\exp(-\sigma^2 k_c^2/2) = 10^{-3}, \tag{62}$$

which leads to

$$\sigma = \frac{3.72}{k_c}. \tag{63}$$

The critical wave number k_c valid for the computation of quasi-wake function is:

$$\exp(-\sigma_r^2 k_c^2/2) = \begin{cases} 10^{-(6-3)} = 10^{-3} & \text{(for single precision)}, \\ 10^{-(12-3)} = 10^{-9} & \text{(for double precision)}, \end{cases} \tag{64}$$

which leads to

$$k_c = \begin{cases} \dfrac{3.72}{\sigma_r} & \text{(for single precision)} \\ \dfrac{6.44}{\sigma_r} & \text{(for double precision).} \end{cases} \tag{65}$$

On the other hand, where σ_s is designated as the applicable rms bunch length in the short-bunch method, σ_s is

$$\sigma_s \cong 5\sigma_r \tag{66}$$

for the same mesh size as in the case of a quasi-wake function in the finite mesh code which computes the reference wake potential. Equations (63), (65) and (66) lead to the following relations for σ, σ_r and σ_s:

$$\sigma = \begin{cases} \sigma_r \cong \dfrac{\sigma_s}{5.0} & \text{(for single precision)} \\ \dfrac{\sigma_r}{1.74} \cong \dfrac{\sigma_s}{8.7} & \text{(four double precision).} \end{cases} \tag{67}$$

Equation (67) indicates that the short-bunch method requires a smaller mesh size by 5.0 or 8.7 times than that used for the quasi-wake function under the condition of $\sigma_s = \sigma$. Compared to the short-bunch method, the use of the quasi-wake function reduces the computing time by a factor of $5.0^3 - 8.7^3$, i.e., about $100 - 600$ in a two-dimensional wake field analysis, and by a factor of $5.0^4 - 8.7^4$, i.e., about 600–5600 in a three-dimensional one. Under the same reference bunch length, the double-precision computation requires only about 10% more computing time than the single-precision one.

4. EXAMPLE OF QUASI-WAKE FUNCTION

The longitudinal quasi-wake function can be applied to a reentrant rf accelerating cavity as shown in Fig. 7. The (longitudinal) reference wake potential is shown in Fig. 8 when a Gaussian bunch passes through the cavity along the central axis with the velocity of light, the rms bunch length $\sigma_r = 5$ cm and $N_\sigma = 4$. The referential wake potential is computed by the finite integration method which is used in the wake field analysis code TBCI.[13]

The frequency of 3 GHz leads to $u_c = 2.22$. Figure 9 shows the functions $g(\xi, u_c)$ and $g_h(\xi, u_c; \xi_G)$ with $\xi_G = 100$ and $u_c = 2.22$, where $g_h(\xi, u_c; \xi_G)$ is defined as follows (see Eq. (33)):

$$g_h(\xi, u_c; \xi_G) = \frac{\pi\sigma_r}{2^{1/2}c} G_h(T, k_c; T_G). \tag{68}$$

The substitution of the function $g_h(\xi, u_c; \xi_G)$ for $g(\xi, u_c)$ in Eq. (31b) generates the quasi-wake function, which is shown in Fig. 10. Since $\xi_G = 100$ is equivalent to $T_G = 3.5$ m in this case, the quasi-wake function exists later than $T = -T_G =$

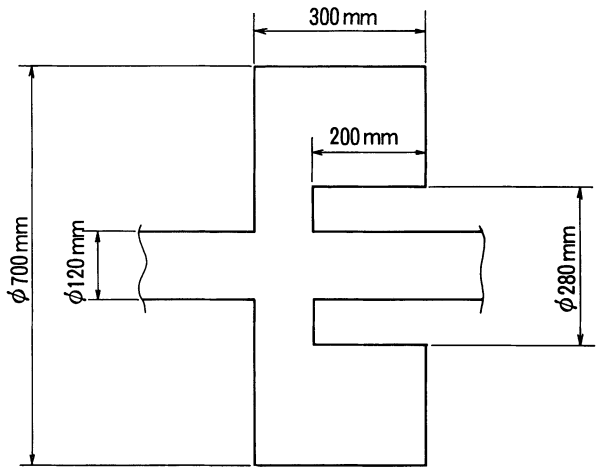

FIGURE 7 Geometry of the reentrant rf accelerating cavity.

-3.54 m. Figure 11 shows the regenerated wake potential with rms bunch length $\sigma = 5$ cm by the quasi-wake function; the result from the short-bunch method is shown for comparison. In this figure, the solid and broken lines indicate the regenerated wake potential and the original one, respectively. The relative error is defined as the ratio of the maximum difference between the regenerated wake potential and the original one to the maximum absolute value of the original one within the Gaussian bunch. The relative error is about 0.1% when using the quasi-wake function, while it is about 20–30% in the short-bunch method, i.e., the use of the quasi-wake function improves the computational accuracy by a factor of 100 compared with the short-bunch method.

Figure 12 shows how the computational accuracy depends on the value of ξ_G for the box-type window and the Hanning-type window cases. In the box-type

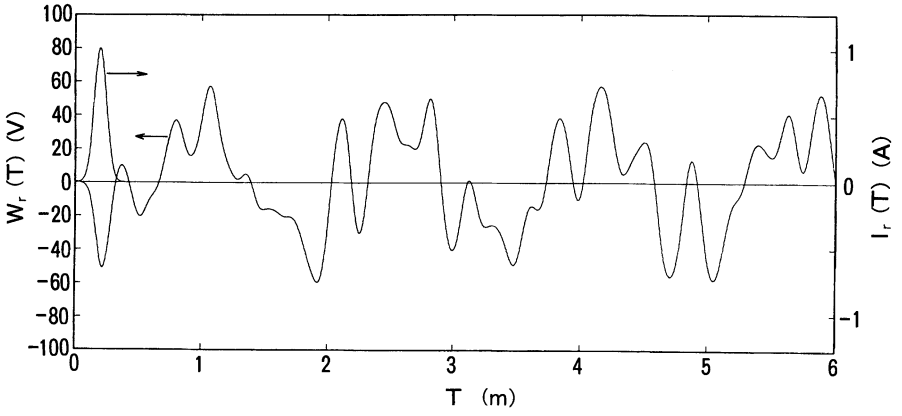

FIGURE 8 Reference wake potential when a Gaussian bunch passes through the cavity (shown in Fig. 7) along the central axis with the velocity of light, RMS bunch length $\sigma_r = 5$ cm, and $N_\sigma = 4$.

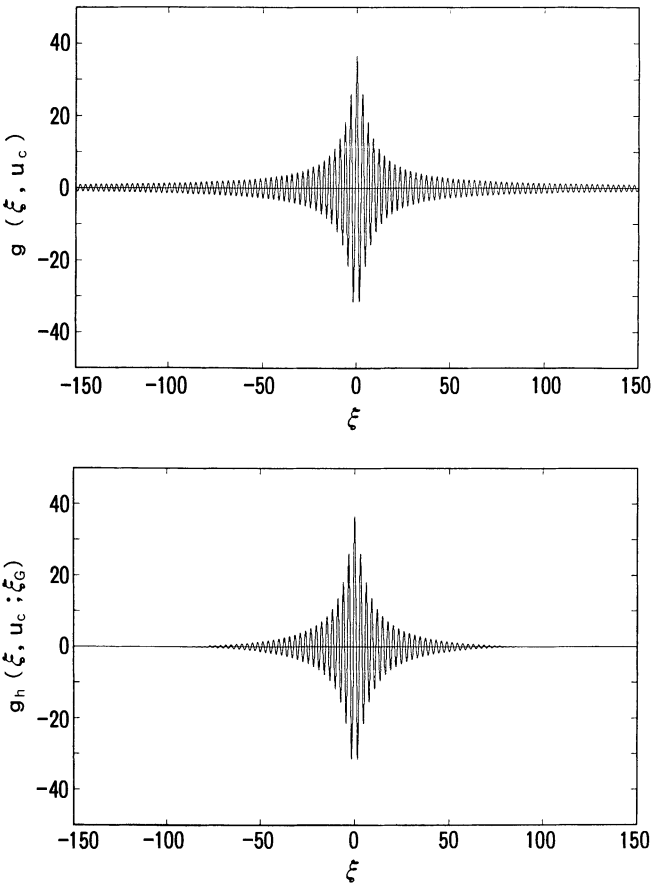

FIGURE 9 Functions $g(\xi, u_c)$ and $g_h(\xi, u_c; \xi_G)$ with $\xi_G = 100$ and $u_c = 2.22$.

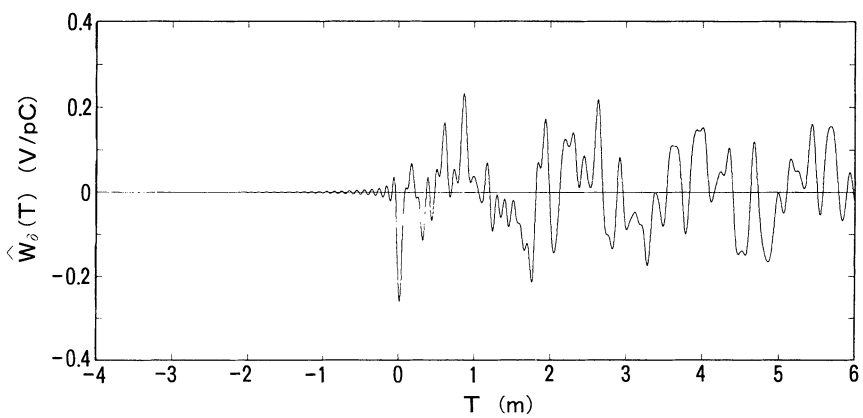

FIGURE 10 Quasi-wake function ($\sigma_r = 5$ cm, $N_\sigma = 4$, and $u_c = 2.22$; critical frequency 3 GHz).

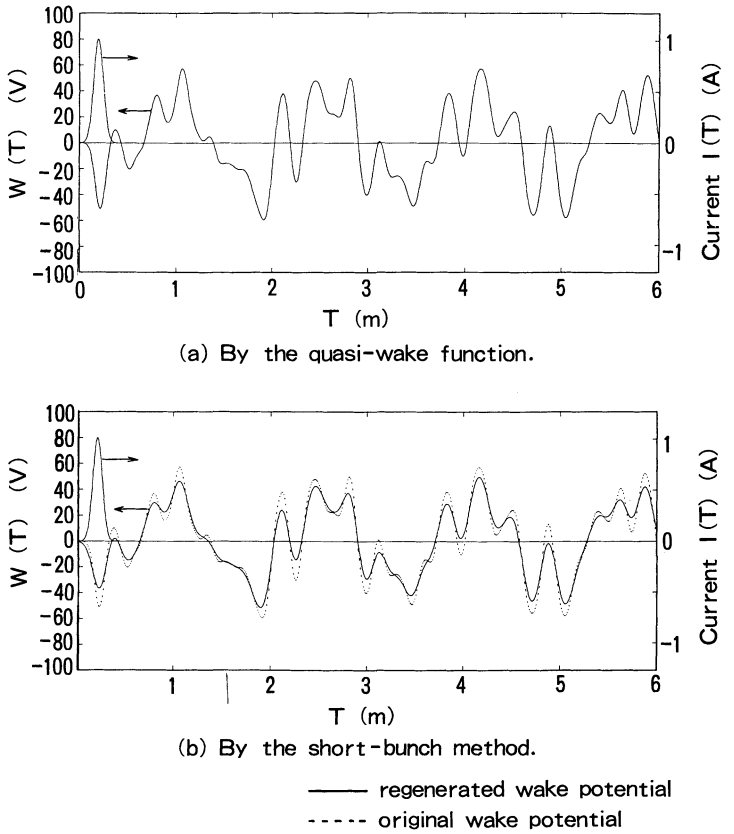

FIGURE 11 Regenerated wake potentials with RMS bunch length $\sigma = 5$ cm by the quasi-wake function and by the short-bunch method.

window, the relative error is about 10–20% with $\xi_G = 100$–150, and it is not reduced below 1% unless ξ_G is extremely large. In the Hanning-type window, the relative error is reduced below 1% with $\xi_G = 30$, and is about 0.1% with $\xi_G = 100$, which is the best possible value; the relative error cannot be further reduced by choosing $\xi_G > 100$. The optimal value of ξ_G varies in accordance with Eq. (50).

5. ANALYSIS OF COUPLING IMPEDANCE BY MAKING USE OF THE QUASI-WAKE FUNCTION

The quasi-wake function is found to serve as Green's function with high accuracy, so it is expected that the quasi-coupling impedance obtained by the Fourier transform of the quasi-wake function gives a good approximation of the exact one. It is important to obtain the coupling impedance since it plays an important role in the analysis of beam instabilities in the frequency domain.

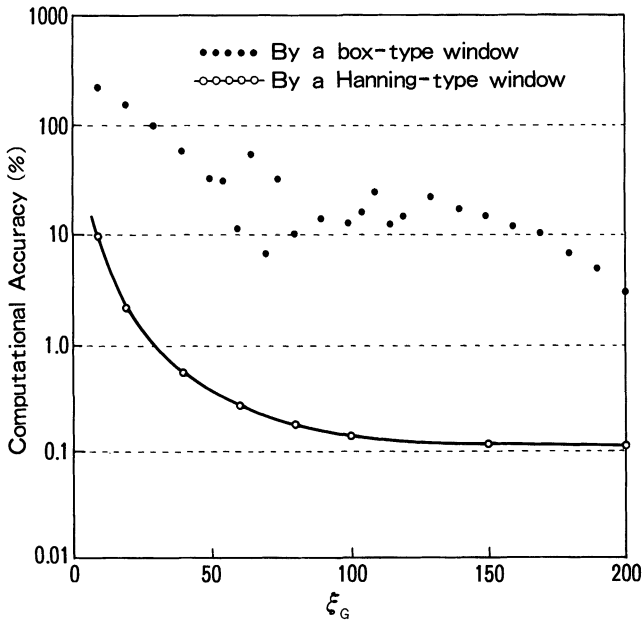

FIGURE 12 ξ_G-dependence of the computational accuracy of regenerated wake potential of a Gaussian bunch with $\sigma = \sigma_r = 5$ cm, critical frequency 3 GHz ($u_c = 2.22$). The result shows two cases using quasi-wake functions by the box-type window and the Hanning-type window for function $G(k, k_c)$.

The coupling impedance can be obtained from the Fourier transform of wake function[14], and it is defined by Eq. (26). The resonator wake is expressed in Eq. (15). It should be noted that Eq. (15) is the result obtained through the exact calculation of Eq. (26). Apparently the numerical calculation of integration up to a positive infinite time cannot be executed in the case of a general wake function. Therefore, in order to obtain a high-accuracy solution in the actual Fourier transform, the domain of integration $\{T \mid -\infty \leqq T \lesssim 5\tau\}$ is substituted for $\{T \mid -\infty \leqq T \leqq \infty\}$, where τ is the damping distance of the resonant mode in meters, as given by:

$$\tau = \frac{2Q}{k_r}, \tag{69}$$

with k_r the resonant wave number. The domain of the integration $\{T \mid -\infty \leqq T \lesssim 5\tau\}$ can surely be used in the broadband resonant mode above the cutoff frequency because $Q \sim 1$–10. However, even the integration of this domain is difficult to execute consistently in the narrowband resonant mode below the cutoff frequency because $Q \sim 10^3$–10^4, which leads to $\tau = 10^3$–10^4 m. This requires a computing time of 100 hours with scalar-type computation using the HITAC-M200H computer, even in a cylindrically symmetric two-dimensional analysis.

Accordingly, $Z_c(k)$ is defined as follows, discriminated from $Z(k)$:

$$Z_c(k) = \frac{1}{c}\int_{-\infty}^{T_m} W_\delta(T)e^{-jkT}\,dT \tag{70a}$$

$$= Z(k)\Gamma(k), \tag{70b}$$

where

$$\Gamma(k) = 1 - \exp\left[-(\gamma + jk)T_m\right]\left[\cos\chi + j\frac{\sin\chi}{S}\left(\frac{k_r}{k} + \frac{j}{2Q}\right)\right], \tag{71}$$

$$\chi = Sk_rT_m, \tag{72}$$

$$\gamma = \frac{1}{\tau}. \tag{73}$$

When $Q > 10$ and $k = k_r$, $\Gamma(k)$ is approximated as follows:

$$\Gamma(k) = 1 - \exp(-\gamma T_m), \tag{74}$$

which leads to

$$Z_c(k_r) = \begin{cases} \dfrac{R}{Q}\left(\dfrac{k_rT_m}{2}\right) & (\text{for } \tau \gg T_m) \\ R & (\text{for } \tau \ll T_m), \end{cases} \tag{75a, 75b}$$

where Eq. (75b) is also applicable to the case of $Q < 10$. Equation (75) implies that the value of R/Q is obtained for the narrowband mode below the cutoff frequency, and the value of R is obtained for the broadband mode above the cutoff frequency.

Since the direct calculation of Eq. (70) requires a wide domain of integration in order to have enough mode separations, the integrand of Eq. (70) is also multiplied by a Hanning-type window $H_h(T, T_m)$. When the integration using the window is defined as $\hat{Z}_c(k)$, it should be noted that $\hat{Z}_c(k)$ is transformed as follows:

$$\hat{Z}_c(k) = Z_c(k) * \bar{H}_h(k, k_m) \tag{76a}$$

$$= \tfrac{1}{2}[Z_c(k) + \tfrac{1}{2}Z_c(k + k_m) + \tfrac{1}{2}Z_c(k - k_m)], \tag{76b}$$

where

$$k_m = \frac{2\pi}{T_m}. \tag{77}$$

Since in a high-Q rf cavity with $Q \geqslant 10^4$, the mode separation of the narrow-band mode is nearly perfect, and no other mode exists exactly at the wave number $k_r \pm k_m$, Eq. (76) is rewritten as follows:

$$\hat{Z}_c(k_r) = \tfrac{1}{2}Z_c(k_r) \quad (\text{for narrowband mode}), \tag{78}$$

which leads to

$$\hat{Z}_c(k_r) = \begin{cases} \dfrac{R}{Q}\left(\dfrac{k_rT_m}{4}\right) & (\text{for } \tau \gg T_m) \\ R & (\text{for } \tau \ll T_m). \end{cases} \tag{79a, 79b}$$

TABLE II

Parameters of Resonator Wake

Resonant frequency (MHz)		$R(\Omega)$	Q	R/Q (Ω)
Narrow band	200.0	∞	∞	100.0
	500.0	∞	∞	100.0
	900.0	∞	∞	100.0
	1300.0	∞	∞	100.0
	1700.0	∞	∞	100.0
	1912.4	(cutoff frequency)		
Broad band	2300.0	100.0	10.0	10.0
	2700.0	100.0	10.0	10.0

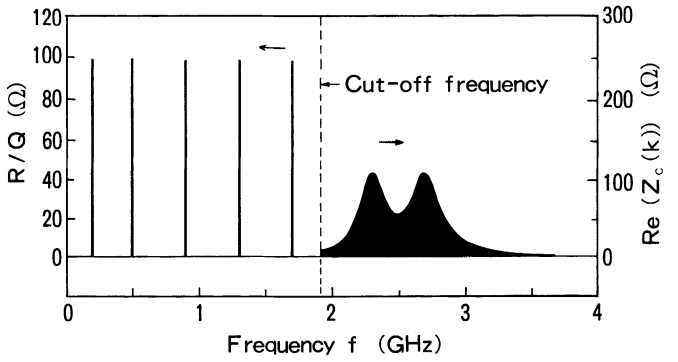

(a) By exact wake function

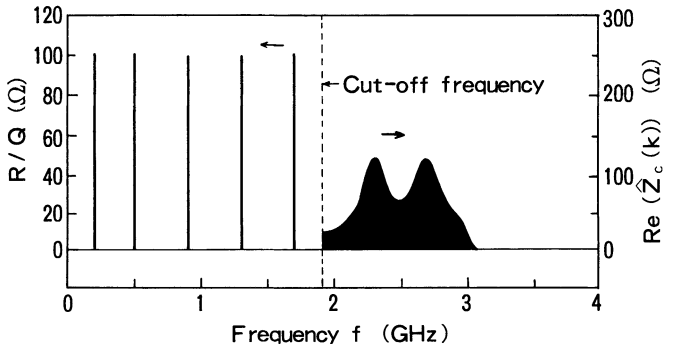

(b) By quasi-wake function

FIGURE 13 R/Q of narrowband modes, and real parts of $Z_c(k)$ and $\hat{Z}_c(k)$ of broadband modes of resonator wake shown in Table 2 with critical frequency 3 GHz.

TABLE III

Resonant Frequencies, R/Q of Narrowband Modes Obtained by Fourier Transform of Quasi-Wake Function, and Computational Errors.

Resonant frequency (MHz)			R/Q (Ω)		
calculated	exact	error (%)	calculated	exact	error (%)
199.68	200.0	−0.159	100.69	100.00	0.69
499.89	500.0	−0.022	99.97	100.00	−0.03
899.96	900.0	−0.004	99.70	100.00	−0.30
1299.99	1300.0	−0.001	99.48	100.00	−0.52
1700.02	1700.0	0.001	99.31	100.00	−0.69

The case is exemplified where Eq. (79) is applied to the resonator wake, the parameters of which are summarized in Table 2. Figure 13 shows R/Q of narrowband modes, along with real parts of $Z_c(k)$ and $\hat{Z}_c(k)$ of broadband modes of the resonator wake, computed both by the exact and quasi-wake functions, with the critical frequency 3 GHz. Table 3 shows the numerical values of the resonant frequencies and R/Q of narrowband modes computed by the quasi-wake function. These results indicate that Eq. (79) give precise values of R/Q for narrowband modes and a rough estimate of R for broadband modes.

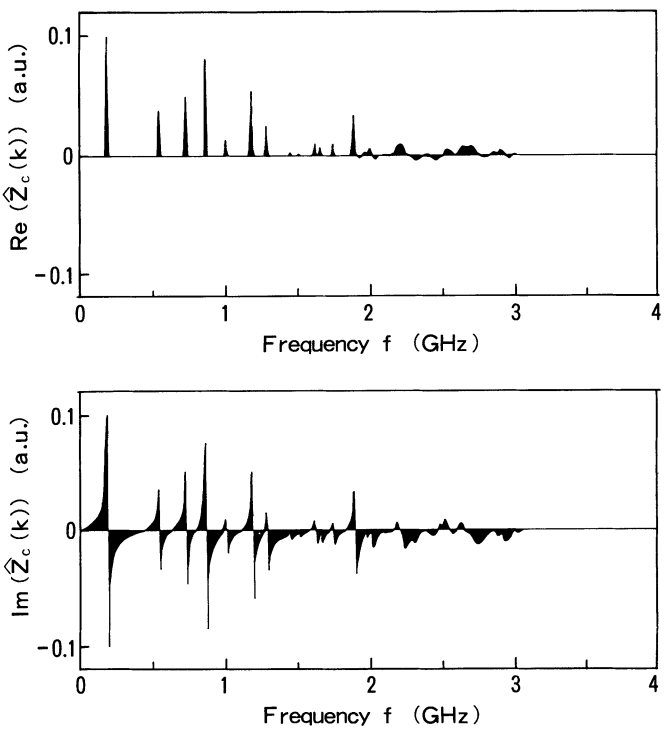

FIGURE 14 Real and imaginary parts of $\hat{Z}_c(k)$ of the reentrant rf accelerating cavities shown in Fig. 7 with critical frequency 3 GHz.

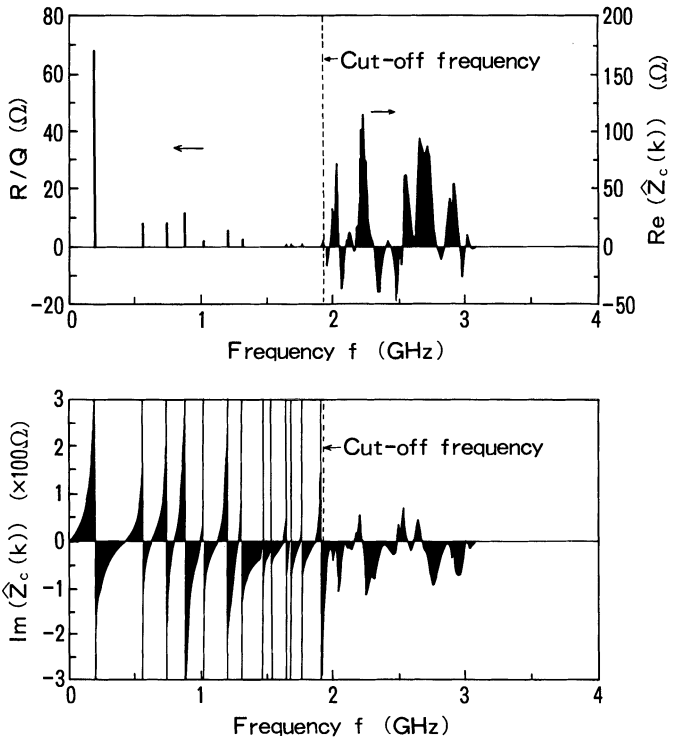

FIGURE 15 Real and imaginary parts of $Z_c(k)$ of the reentrant rf accelerating cavities shown in Fig. 7 with critical frequency 3 GHz. For narrowband modes below the cut-off frequency 1.91 GHz, R/Q values are shown instead of the real part of $Z_c(k)$. R values can be read for the broadband modes. The spectra below the cutoff frequency are refined considering the Q values of infinity.

The analysis of R/Q and R performed with Eq. (79) is applied to the quasi-wake function of the perfect conducting rf cavity shown in Fig. 7. Figure 14 shows the real and imaginary parts of $\hat{Z}_c(k)$ of the rf cavity with the critical frequency 3 GHz and with the upper limit value of the domain of integration $T_m = 20$ m. Figure 15 shows the values of R/Q and R obtained from the real part of $\hat{Z}_c(k)$ and the imaginary part of $\hat{Z}_c(k)$ where the spectra below the cut-off

TABLE IV

Comparison of Calculations Between Quasi-Wake Function and SUPERFISH with Respect to Resonant Frequencies and R/Q of Narrowband Modes.

Resonant frequency (MHz)			R/Q (Ω)		
quasi-wake function	SUPERFISH	error (%)	quasi-wake function	SUPERFISH	error (%)
190.19	191.69	−0.783	68.76	68.95	−0.28
546.22	546.78	−0.102	8.45	8.26	2.30
729.30	730.46	−0.159	8.80	8.57	2.68
867.21	869.31	−0.242	12.10	11.54	4.85

frequency are refined considering the Q values of infinity. The negative real components of the broadband modes above the cut-off frequency are ascribed to numerical errors in the referential wake potential.

The resonant frequencies and R/Q for narrowband modes below the cut-off frequency are also obtained by the electromagnetic resonant field analysis code SUPERFISH. Table 4 lists the computational results obtained both by the quasi-wake function and SUPERFISH. It is confirmed that the two methods agree well with each other, having relative errors of 0.1%–0.8% in resonant frequency of several percent in R/Q.

6. CONCLUSIONS

The quasi-wake function is presented as an approximate kernel function in the convolution integral for the wake potential. The quasi-wake function is computed from the convolution integral of a reference wake potential of a Gaussian bunch and the kernel function $G(T, k_c)$ multiplied by the Hanning-type window. The maximum length of the reference Gaussian bunch can be equal to the applicable bunch length in the single-precision computation of reference wake potential, while in the double precision computation the former can be longer than the latter by a factor of 1.7. Compared with the short-bunch method, which is one conventional approach, the quasi-wake function requires a computing time shorter by a factor of 600 in the two-dimensional wake field analysis and by a factor of 5600 in the three-dimensional wake field analysis. The Fourier transform of the quasi-wake function gives resonant frequencies and R/Q of the narrow-band modes with high computational accuracy, along with a rough estimate of R for the broadband modes.

ACKNOWLEDGMENTS

The authors would like to thank the members of the Accelerator Code Group at Los Alamos National Laboratory for the use of SUPERFISH. The authors also appreciate the continuous encouragement offered by Dr. T. Ohmae on this research.

REFERENCES

1. A. W. Chao, Coherent Instabilities of a Relativistic Bunched Beam, SLAC-PUB 2946 (1982).
2. K. Halbach and R. F. Holsinger, *Particle Accelerators* **7,** 213 (1976).
3. H. Henke, Electromagnetic Interaction between Charged-Particle Beams and Environment, CERN/LEP-RF/86-21 (1986).
4. T. Weiland, On the Quantitative Prediction of Bunch Lengthening in High Energy Electron Storage Rings, DESY 81-088 (1981).
5. D. Brandt and B. Zotter, Calculation of the Wakefield with the Optical Resonator Model, CERN-ISR/TH/82-13 or LEP Note 388 (1982).
6. E. Keil, *Nucl. Instrum. Methods* **100,** 419 (1972).

7. K. Bane, "Constructing the Wake Potentials from the Empty Cavity Solutions at Maxwell's Equations," CERN/ISR-TH/80-47 (1980).
8. K. Bane, Wakefield Effects in a Linear Collider, SLAC PUB-4169 (1986) or K. Bane, in M. Month and M. Dienes, Eds., Physics of Particle Accelerators, AIP Conf. Proc. No. 153 Vol. 1 (Am. Inst. Phys., New York, 1987), p. 971.
9. B. Zotter, The Equivalent Broad-Band Impedance in LEP: Updated Estimates of the Current Thresholds due to Transverse Mode-Coupling, CERN LEP-TH/87-34 (1987).
10. K. Bane and P. B. Wilson, Proceedings of the 11th Int. Conf. on High-Energy Accelerators, CERN, Geneva (Birkhauser Verlag, Basel, 1980), p. 592.
11. D. Brandt, Simulation of Longitudinal Single-Bunch Effects in LEP, CERN-ISR/TH/82-09 (1982).
12. R. B. Blackman and J. W. Tukey, The Measurement of Power Spectra from the Point of View of Communication Engineering, Dover Publications, Inc. (1958).
13. T. Weiland, CERN/ISR-TH/80-46 (1980).
14. For example, K. Bane and R. Ruth (p. 10) and J. Bisognano and K. Y. Ng (p. 45) in: "Report of the SSC Impedance Workshop," SSC-SR-1017 (1985).